Approximate Analytical Evaluation of the Continuous Spectrum in a Substrate–Superstrate Dielectric Waveguide

Paolo Baccarelli, *Member, IEEE*, Paolo Burghignoli, *Member, IEEE*, Fabrizio Frezza, *Senior Member, IEEE*, Alessandro Galli, *Member, IEEE*, Giampiero Lovat, *Student Member, IEEE*, and David R. Jackson, *Fellow, IEEE*

***Abstract*—In this paper, an original closed-form approximate evaluation is performed for the continuous-spectrum field excited by an infinite line source in a dielectric substrate–superstrate configuration, optimized for leaky-wave radiation. By means of a suitable approximate asymptotic representation obtained via Watson's lemma, the continuous-spectrum field has been expressed as the sum of the contributions of two leaky-pole singularities, each weighted by a transition function that depends on both the frequency and observation distance. The validity of these results is shown in the near and far fields at different frequencies, including the frequency range in which the leaky wave is physical and the entire transition region through the spectral gap. This new closed-form result explicitly shows the nature of the continuous-spectrum field in the transition region, and provides insight into the nature of the fields on more complicated structures in microwave integrated circuits.**

***Index Terms*—Continuous spectrum, dielectric waveguides, leaky waves (LWs), transition regions.**

I. Introduction and Background

As IS KNOWN, radiation due to sources in the presence of open waveguides can be described in terms of the continuous part of the modal spectrum of the relevant transverse operator (see, e.g., [1]–[4]). Such a description is exact, but requires the numerical determination of the continuous-spectrum modes, which is a quite cumbersome task.

In many cases, the exact modal representation can be conveniently replaced by an approximate one in terms of leaky waves (LWs), i.e., modal solutions with a complex propagation constant that propagate and simultaneously leak energy through waves supported by the background environment of the waveguide (e.g., plane waves in free space or surface waves in a planar-stratified structure). Such leaky modes do not satisfy the radiation conditions at infinity in the waveguide transverse cross section; nevertheless, when a leaky mode is physical, its field can give an accurate representation of the continuous-spectrum field excited by a given source [5]–[8].

The part of the continuous spectrum that is not represented by the LW field, termed the *residual wave* (RW) in [9], has recently been studied for the three-dimensional case of a stripline excited by a gap source in [10]. The residual-wave contribution to the field typically becomes strong in the neighborhood of the transition region, where the leaky mode evolves from a physical to nonphysical mode [11], [12]. As the leaky mode moves into the nonphysical region, the degree of correlation between the LW field and continuous-spectrum field gradually decreases [13]. A quantitative description is sought for this progressive loss of physical significance of a leaky mode; thus far, empirical weighting functions have been proposed, based on power considerations [14], but, to our knowledge, no analytically derived results are as yet available.

In this paper, we consider a simple two-dimensional configuration, i.e., a substrate–superstrate dielectric waveguide excited by an infinite line source and optimized for LW radiation [15], [16]. This structure is chosen for its simplicity. However, the conclusions obtained are expected to be valid for more complicated structures such as sources on microwave-integrated-circuit lines. Hence, the analysis and results presented here should provide insight into the nature of the continuous-spectrum radiation at high frequencies on practical integrated-circuit lines, which is often responsible for undesirable spurious effects.

By means of an asymptotic evaluation performed via Watson's lemma [17], we present an approximate closed-form expression for the residual-wave field on the air–dielectric interface, which leads to a closed-form expression for the continuous-spectrum field in terms of the contribution of *two* poles of the spectral Green's function, each weighted by an appropriate *transition function*. The results thus obtained, reported here for both the near and far fields, explicitly show the nature of the continuous-spectrum field in the neighborhood of the transition region of the substrate–superstrate dielectric waveguide.

This paper is organized as follows. In Section II, the analytical derivation of the approximate closed-form expression for the RW is derived for a substrate–superstrate dielectric waveguide excited by an electric line source and optimized for TE LW radiation. In Section III, the results thus obtained are used to derive an approximate representation of the continuous-spectrum field in terms of two weighted LW pole contributions. In Section IV, numerical results are presented for both the aperture and radiated far fields, and a comparison is presented with the results obtained through the use of the empirical transition function of [14]. Finally, in Section V, conclusions are presented.

Manuscript received April 5, 2002; revised August 10, 2002.

P. Baccarelli, P. Burghignoli, F. Frezza, A. Galli, and G. Lovat are with the Department of Electronic Engineering, "La Sapienza" University of Rome, 00184 Rome, Italy (e-mail: baccarelli@die.uniroma1.it).

D. R. Jackson is with the Department of Electrical and Computer Engineering, University of Houston, Houston, TX 77204-4005 USA.

Digital Object Identifier 10.1109/TMTT.2002.805132

0018-9480/02$17.00 © 2002 IEEE

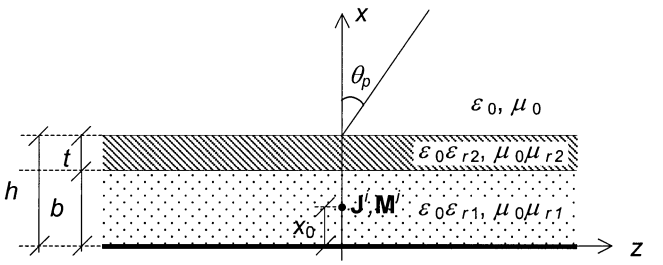

Fig. 1. Substrate–superstrate configuration treated here, excited by an infinite line source that may be electric ($\mathbf{J}^i$) or magnetic ($\mathbf{M}^i$).

II. Approximate Evaluation of the Residual-Wave Field

The two-layer substrate–superstrate planar waveguide considered here is shown in Fig. 1, where b is the substrate height, t is the superstrate height, and ε_{r1}, μ_{r1} and ε_{r2}, μ_{r2} are the relative permittivities and permeabilities of the substrate and superstrate, respectively; the infinite line source is directed along the y-axis, and is placed at $z = 0$ at a distance x_0 above the ground plane. This structure was proposed as an antenna geometry capable of producing narrow radiated beams, when the dimensions and constitutive parameters of both the substrate and superstrate are chosen properly [15]. Its behavior has subsequently been interpreted as due to the excitation of LWs supported by the structure [16].

The invariance of both the structure and excitation with respect to the y-direction allows us to study the TE and TM polarizations separately. In this paper, we will be concerned with the TE polarization (due to an electric-line-source excitation); however, the same approach can be used to treat the TM case as well (due to a magnetic-line-source excitation).

In the TE case, an electric line source is present, which excites an electromagnetic field with nonzero components E_y, H_x, and H_z. The following high-gain conditions [15] are chosen to optimize the design:

$$\begin{aligned} k_0 b\sqrt{\mu_{r1}\varepsilon_{r1} - \sin^2\theta_p} &= \pi \\ k_0 t\sqrt{\mu_{r2}\varepsilon_{r2} - \sin^2\theta_p} &= \frac{\pi}{2} \\ x_0 &= \frac{b}{2} \end{aligned} \tag{1}$$

where k_0 is the free-space wavenumber and $\varepsilon_{r2} \gg 1$ in order to obtain a directive beam at an angle θ_p, due to radiation from the first higher order TE mode (TE_2 leaky mode) [16].

The electromagnetic field at each point in space can be derived from the knowledge of the electric field on the air–dielectric interface ($x = h$); the latter can be expressed as an inverse Fourier transform as

$$\mathbf{E}(h,z) = \mathbf{y}_0 E_y(h,z) = \mathbf{y}_0 \frac{1}{2\pi}\int_{-\infty}^{+\infty} \tilde{G}_{yy}(h;k_z)e^{-jk_z z}dz \tag{2}$$

where the integral is performed along the real axis, assuming infinitesimal losses. The spectral Green's function $\tilde{G}_{yy}$ occurring in (2) is known in a simple closed form [7]:

$$\tilde{G}_{yy}(h;k_z) = -\omega\mu_0 \frac{\dfrac{k_{x2}\sin(k_{x1}x_0)}{k_{x2}\sin(k_{x1}b)\cos(k_{x2}t) + k_{x1}\cos(k_{x1}b)\sin(k_{x2}t)}}{k_{x0} + jk_{x2}\dfrac{k_{x2}\tan(k_{x1}b) - jk_{x1}\cot(k_{x2}t)}{k_{x1} + k_{x2}\tan(k_{x1}b)\cot(k_{x2}t)}} \tag{3}$$

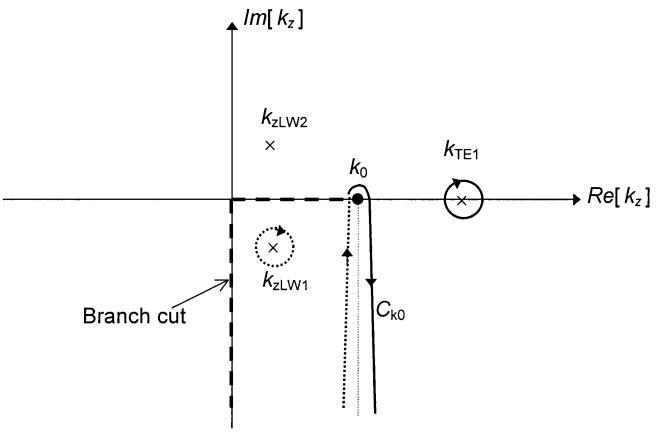

Fig. 2. Location of the singularities of the Green's function in the complex k_z-plane. k_{TE1}: proper (TE_1) surface-wave pole, $k_{z\mathrm{LW1}}$: LW (TE_2) improper complex pole, $k_{z\mathrm{LW2}}$: improper complex pole (the complex-conjugate of the $k_{z\mathrm{LW1}}$ pole), k_0: branch point. The SDP C_{k0} lies partly on the improper Riemann sheet (dotted line), and partly on the proper Riemann sheet (solid line), which are separated by a branch cut (dashed line).

where $k_{x0} = \sqrt{k_0^2 - k_z^2}$, $k_{x1} = \sqrt{\varepsilon_{r1}k_0^2 - k_z^2}$, and $k_{x2} = \sqrt{\varepsilon_{r2}k_0^2 - k_z^2}$ are the transverse wavenumbers in the air, substrate, and superstrate, respectively, assuming nonmagnetic layers.

The spectral Green's function $\tilde{G}_{yy}$ has pole singularities, which correspond to the discrete modes of the substrate–superstrate structure, and branch-point singularities at $k_z = \pm k_0$ [7]. These branch points are due to the square-root function occurring in the definition of the transverse wavenumber in air. The choice of the square root with a negative imaginary part corresponds to waves attenuating at infinity, and is termed *proper*, while the other determination is termed *improper*. The original path stays on the proper sheet of the k_z-plane. By deforming the integration path in (2) in the lower half-plane (for $z > 0$) around the Sommerfeld branch cut that separates the proper (*top*) and improper (*bottom*) Riemann sheets (see Fig. 2), the total field (TF) on the interface can be expressed as the sum of the following terms: the residue contribution of the captured proper poles on the real axis, which constitutes the bound-mode field (in our case, the field of the TE_1 mode) and the contribution of the integral around the branch cut, which constitutes the continuous-spectrum field. By further deforming the integration path to the steepest descent path (SDP) (the vertical path C_{k0} that goes around the k_0 branch point in Fig. 2) [6], the continuous spectrum can be expressed as the sum of the residue contribution of the captured (physical) leaky poles (in our case, the TE_2 mode, neglecting the higher order leaky modes) and the contribution of the integral around C_{k0}, which constitutes the residual-wave field [9], [10] (called the space-wave field in [14]). The above-described field decomposition can be written as (for $z > 0$)

$$\begin{aligned} E_y(h,z) = &-j\mathrm{Res}\left[\tilde{G}_{yy}(h;k_z)\right]_{k_z=k_{\mathrm{TE}_1}} e^{-jk_{\mathrm{TE}_1}z} \\ &+ -j\mathrm{Res}\left[\tilde{G}_{yy}(h;k_z)\right]_{k_z=k_{z\mathrm{LW1}}} e^{-jk_{\mathrm{LW1}}z} \\ &\times\left\{1 - u_{-1}\left[\Re\mathrm{e}\left[k_z - k_0\right]\right]\right\} + E_{\mathrm{RW}}(h,z) \end{aligned} \tag{4}$$

where k_{TE1} is the TE_1 surface-wave pole, $k_{z\mathrm{LW1}}$ is the TE_2 LW pole; the unit-step function u_{-1} is equal to zero

when $k_{z\mathrm{LW1}}$ is captured (the leaky mode is physical with $\beta_{z\mathrm{LW1}} = \Re e[k_{z\mathrm{LW1}}] < k_0$) and is equal to one when it is not (the leaky mode is in the nonphysical region where $\beta_{z\mathrm{LW1}} > k_0$), and the residual-wave field E_{RW} is given by

$$E_{\mathrm{RW}}(h,z) = \frac{1}{2\pi}\int_{C_{k_0}} \tilde{G}_{yy}(h;k_z)e^{-jk_z z}dk_z. \tag{5}$$

Later on, the dependence on h will be omitted in all the relevant symbols.

By performing the change of variable $k_z = k_0 - js$ in (5), after some manipulations, we obtain

$$E_{\mathrm{RW}}(z) = -\frac{e^{-jk_0 z}}{2\pi}\int_0^{+\infty} F(s)e^{-sz}ds \tag{6}$$

where the resulting integrand $F(s) = F^+(s) - F^-(s)$ is the difference of the original $\tilde{G}_{yy}$ calculated on the two parts of the C_{k_0} path, the proper ($F^+(s)$), and the improper ($F^-(s)$) parts.

To achieve an approximate analytical expression for the residual-wave field, we let s tend to zero in order to obtain an asymptotic approximation for large z. Based on this assumption, the following approximate form for the Green's function can be obtained:

$$\tilde{G}_{yy}(k_z) = \tilde{G}_{yy}(k_0 - js) \cong \frac{N_0}{D(s)} \tag{7}$$

where N_0 does not depend on s, and $D(s)$ is given by

$$D(s) = s + A_1 s^{1/2} + A_2 \tag{8}$$

where A_1 and A_2 are complex coefficients that depend on the involved physical parameters, including frequency. The choice of the square root depends on the Riemann sheet on which the evaluation of the approximate Green's function is performed. In particular, the approximate transverse wavenumber in air can be written as $k_{x0} \cong (1+j)\sqrt{k_0}s^{1/2}$. Therefore, by examining the sign of the imaginary part of k_{x0}, it is found that, if the following condition holds:

$$-\frac{\pi}{2} \le \mathrm{Arg}(s) < \frac{3\pi}{2} \tag{9}$$

the evaluation of the approximate Green's function is performed on the improper (bottom) Riemann sheet. Hence, the branch cut in the s-plane is chosen to be along the negative imaginary axis. The principal square root $\sqrt{s}$ is then defined to be the value on the bottom sheet, corresponding to (9). Hence, $s^{1/2} = \pm\sqrt{s}$, where the plus sign corresponds to the bottom sheet and the minus sign corresponds to the top sheet.

Based on (7) and (8), the integrand in (6) can then be expressed as

$$\begin{aligned} F(s) &= F^+(s) - F^-(s) \\ &\cong N_0\left[\frac{1}{s - A_1\sqrt{s} + A_2} - \frac{1}{s + A_1\sqrt{s} + A_2}\right] \\ &= N_0\left[\frac{2A_1\sqrt{s}}{s^2 + s\,(2A_2 - A_1^2) + A_2^2}\right] \\ &= N_0\left[\frac{2A_1\sqrt{s}}{(s-s_1)(s-s_2)}\right] \\ &= A_{\mathrm{res}}\left[\frac{1}{s-s_1} - \frac{1}{s-s_2}\right]\sqrt{s} \end{aligned} \tag{10}$$

where A_{res} is a suitable complex coefficient, while s_1 and s_2 are the locations of the poles of the approximate layered Green's function in the two-sheeted s-plane, corresponding to the poles $k_{z\mathrm{LW1}}$ and $k_{z\mathrm{LW2}}$, shown in Fig. 2, respectively, as

$$\begin{aligned} k_{z_{\mathrm{LW1}}} &\cong k_0 - js_1 \\ k_{z_{\mathrm{LW2}}} &\cong k_0 - js_2. \end{aligned} \tag{11}$$

By inserting (10) in (6), we obtain

$$E_{\mathrm{RW}}(z) \cong -jA_{\mathrm{res}}\frac{e^{-jk_0 z}}{2\pi}\int_0^{+\infty}\left(\frac{\sqrt{s}}{s-s_1} - \frac{\sqrt{s}}{s-s_2}\right)e^{-sz}ds. \tag{12}$$

The integral in this expression can be evaluated analytically in a closed form (see the Appendix). The result is

$$\begin{aligned} E_{\mathrm{RW}}(z) &\cong \frac{A_{\mathrm{res}}}{2}e^{-jk_0 z}\Big\{\sqrt{s_1}e^{-s_1 z}\Big[\mathrm{Sgn}\big[\Im m[s_1]\big] + \mathrm{Erf}\big(j\sqrt{s_1 z}\big)\Big] \\ &\quad - \sqrt{s_2}e^{-s_2 z}\Big[1 + \mathrm{Erf}\big(j\sqrt{s_2 z}\big)\Big]\Big\} \end{aligned} \tag{13}$$

where the imaginary part of the s_1 pole changes its sign when the $k_{z\mathrm{LW1}}$ pole crosses the C_{k_0} path in the k_z-plane.

Through the asymptotic expansion of the Erf function for large values of its argument, it can be shown that the residual-wave approximate expression of (13) has an algebraic decay for large z, which is proportional to $z^{-3/2}$ if both poles s_1 and s_2 are different from zero; if one of the two poles is equal to zero, the algebraic decay is instead proportional to $z^{-1/2}$. The latter case occurs at cutoff of the TE_2 mode. These conclusions are in agreement with those obtained by applying Watson's lemma to (6) [10].

III. Approximate Continuous Spectrum (ACS) Field and Leaky-Wave Transition Functions

On the basis of the results derived in Section II, it is possible to obtain an approximate expression for the *entire continuous-spectrum* field on the air–superstrate interface. The ACS field can be obtained by summing the LW field of the $k_{z\mathrm{LW1}}$ pole (when captured) and the approximate residual wave (ARW) field of (13).

The LW field E_{LW1} of the $k_{z\mathrm{LW1}}$ pole is given by (for $z > 0$)

$$E_{\mathrm{LW1}}(z) = -j\mathrm{Res}\left[\tilde{G}_{yy}(k_z)\right]_{k_z = k_{z\mathrm{LW1}}} e^{-jk_{\mathrm{LW1}}z}. \tag{14}$$

Now, by assuming that (11) is valid, i.e., that the poles of the approximate algebraic expression accurately represent the actual poles of the exact Green's function $\tilde{G}_{yy}$, the residue contribution from the $k_{z\mathrm{LW1}}$ pole can be expressed as

$$\begin{aligned} -j\mathrm{Res}\left[\tilde{G}_{yy}(k_z)\right]_{k_z = k_{z\mathrm{LW1}}} &\cong -\mathrm{Res}\left[F^-(s)\right]_{s=s_1} \\ &= \mathrm{Res}\left[F(s)\right]_{s=s_1}. \end{aligned} \tag{15}$$

From (10), we then have

$$-j\mathrm{Res}\left[\tilde{G}_{yy}(k_z)\right]_{k_z = k_{z\mathrm{LW1}}} \cong A_{\mathrm{res}}\sqrt{s_1}. \tag{16}$$

Therefore, the LW field of the $k_{z\mathrm{LW1}}$ pole can be written as

$$E_{\mathrm{LW1}}(z) \cong A_{\mathrm{res}}\sqrt{s_1}e^{-j(k_0 - js_1)z}. \tag{17}$$

With similar steps, the LW field of the $k_{z\mathrm{LW}2}$ pole can be written as

$$E_{\mathrm{LW}2}(z) = -j\mathrm{Res}\left[\tilde{G}_{yy}(k_z)\right]_{k_z=k_{z\mathrm{LW}2}} e^{-jk_{z\mathrm{LW}2}z} \cong -A_{\mathrm{res}}\sqrt{s_2}e^{-j(k_0-js_2)z}. \quad (18)$$

Using (4), (13), (17), and (18), and taking into account that Erf is an odd function, the complete ACS field E_{CS} is then obtained as

$$\begin{aligned} E_{\mathrm{CS}}(z) \cong & A_{\mathrm{res}}\sqrt{s_1}e^{-j(k_0-js_1)z} \\ & \times\left\{\left[1-u_{-1}\left[\Im m\left[s_1\right]\right]\right]+\frac{1}{2}\mathrm{Sgn}\left[\Im m\left[s_1\right]\right]\right. \\ & \left.+\frac{1}{2}\mathrm{Erf}\left(j\sqrt{s_1 z}\right)\right\} \\ & -A_{\mathrm{res}}\sqrt{s_2}e^{-j(k_0-js_2)z}\left[\frac{1}{2}+\frac{1}{2}\mathrm{Erf}\left(j\sqrt{s_2 z}\right)\right] \\ = & A_{\mathrm{res}}\sqrt{s_1}e^{-j(k_0-js_1)z}\left[\frac{1}{2}+\frac{1}{2}\mathrm{Erf}\left(j\sqrt{s_1 z}\right)\right] \\ & -A_{\mathrm{res}}\sqrt{s_2}e^{-j(k_0-js_2)z}\left[\frac{1}{2}+\frac{1}{2}\mathrm{Erf}\left(j\sqrt{s_2 z}\right)\right]. \end{aligned} \quad (19)$$

All of the square roots in this equation denote principal values defined according to (9), as previously mentioned. This expression holds under the assumption that the poles s_1 and s_2 of the approximate function $F(s)$ accurately represent [via (11)] the poles $k_{z\mathrm{LW}1}$ and $k_{z\mathrm{LW}2}$ of the exact Green's function, and also that the relevant approximate residues accurately represent the exact ones. Under these hypotheses, it is then possible to perform the calculation by using the exact values of the poles and their residues in (19). By introducing the transition function

$$T_{\mathrm{LW}}(k_{z\mathrm{LW}i}-k_0,z)=\frac{1}{2}+\frac{1}{2}\mathrm{Erf}\left[j\sqrt{j(k_{z\mathrm{LW}i}-k_0)z}\right], \quad i=1,2 \quad (20)$$

(19) can then be written in terms of the *exact* pole contributions $E_{\mathrm{LW}1}$ and $E_{\mathrm{LW}2}$ as

$$\begin{aligned} E_{\mathrm{CS}}(z) \cong & E_{\mathrm{LW}1}(z)T_{\mathrm{LW}}\left(k_{z\mathrm{LW}1}-k_0,z\right) \\ & +E_{\mathrm{LW}2}(z)T_{\mathrm{LW}}\left(k_{z\mathrm{LW}2}-k_0,z\right) \\ = & W_{\mathrm{LW}1}(z)+W_{\mathrm{LW}2}(z). \end{aligned} \quad (21)$$

We have thus obtained an approximate closed-form expression for the continuous-spectrum field, as a sum of *two* weighted poles contributions, $W_{\mathrm{LW}1}$ and $W_{\mathrm{LW}2}$, each involving the standard transition function in which the Erf function occurs [7]. It should be observed that the same transition function T_{LW} occurs for *both* poles, including $k_{z\mathrm{LW}1}$, which may be captured in the integral-path deformation (it is captured when the pole is physical), and $k_{z\mathrm{LW}2}$, that is never captured. However, the sign difference between the imaginary parts of the two poles makes the two factors $T_{\mathrm{LW}}(k_{z\mathrm{LW}1}-k_0,z)$ and $T_{\mathrm{LW}}(k_{z\mathrm{LW}2}-k_0,z)$ very different, as functions of both frequency f and longitudinal abscissa z. The consideration of the nonphysical pole $k_{z\mathrm{LW}2}$ is necessary, due to the fact that it is close to the k_0 branch point and, therefore, influences the asymptotic evaluation [18], [19].

In the results presented below, the weighted LW expression (21), which approximates the continuous-spectrum field by using the exact pole locations in the evaluation of the transition function, will be compared with the ACS field obtained by summing the exact LW field (when captured) and the ARW field calculated through (13), which uses the approximate (closed-form) expressions s_1 and s_2 for the pole locations. The ACS field is calculated using (13) and the exact LW field instead of using (19) (which approximates the LW field) in order to improve the calculation of the ACS.

Although the above derivation has assumed that $z>0$, the result may be generalized to arbitrary z by replacing z with $|z|$ (this generalization is important for the calculation of the far field).

As is well known, the total radiated far field can be obtained by means of the Fourier transform with respect to z of the total aperture field of (2) as

$$E_{\mathrm{TF}}^{\mathrm{far}}(r,\theta)=\sqrt{\frac{jk_0}{2\pi}}\frac{e^{-jk_0 r}}{\sqrt{r}}\cos\theta\tilde{G}_{yy}\left(k_0\sin\theta\right) \quad (22)$$

where the polar coordinates (r,θ) in the xz-plane have been introduced. The continuous-spectrum component of the near field gives rise to a far-field component, which can again be obtained through its Fourier transform $\tilde{E}_{\mathrm{CS}}(k_z)$ as

$$E_{\mathrm{CS}}^{\mathrm{far}}(r,\theta)=\sqrt{\frac{jk_0}{2\pi}}\frac{e^{-jk_0 r}}{\sqrt{r}}\cos\theta\tilde{E}_{\mathrm{CS}}(k_0\sin\theta). \quad (23)$$

The difference between $E_{\mathrm{TF}}^{\mathrm{far}}$ and $E_{\mathrm{CS}}^{\mathrm{far}}$ is due to the far-field contribution of the bound-wave field, which radiates because of its discontinuous derivative at the source.

By means of [20, eq. 7.4.19], one obtains

$$\begin{aligned} & \int_{-\infty}^{+\infty} e^{-j(k_0-js_i)|z|}\left[\frac{1}{2}+\frac{1}{2}\mathrm{Erf}\left(j\sqrt{s_i|z|}\right)\right]e^{jk_z z}dz \\ & =\frac{1}{2}\left\{\frac{1}{k_0-js_i-k_z}\left[\sqrt{\frac{s_i}{j(k_0-k_z)}}-j\right]\right. \\ & \left.+\frac{1}{k_0-js_i+k_z}\left[\sqrt{\frac{s_i}{j(k_0+k_z)}}-j\right]\right\}. \end{aligned} \quad (24)$$

The Fourier transform of the continuous-spectrum field can then be approximately evaluated in a closed form as

$$\tilde{E}_{\mathrm{CS}}(k_z)\cong\tilde{W}_{\mathrm{LW}1}(k_z)+\tilde{W}_{\mathrm{LW}2}(k_z) \quad (25)$$

where

$$\begin{aligned} \tilde{W}_{\mathrm{LW}i}(k_z) = & \frac{1}{2}\mathrm{Res}\left[\tilde{G}_{yy}(k_z)\right]_{k_z=k_{z\mathrm{LW}i}} \\ & \times\left[\frac{1}{k_z-k_{z\mathrm{LW}i}}\left(1+j\sqrt{\frac{k_{z\mathrm{LW}i}-k_0}{k_0-k_z}}\right)\right. \\ & \left.-\frac{1}{k_z+k_{z\mathrm{LW}i}}\left(1+j\sqrt{\frac{k_{z\mathrm{LW}i}-k_0}{k_0+k_z}}\right)\right] \end{aligned} \quad (26)$$

with $i=1,2$ are the Fourier transforms of the weighted LW aperture fields $W_{\mathrm{LW}i}(z)$.

It can be finally observed that, although the derivation has been carried out by assuming that both of the poles s_1 and s_2 are improper, the same approach can be used to treat the case in which one of the poles is proper (this situation occurs above the cutoff frequency of the TE_2 mode). This allows us to also accurately represent the radiative effects when the TE_2 surface wave is excited.

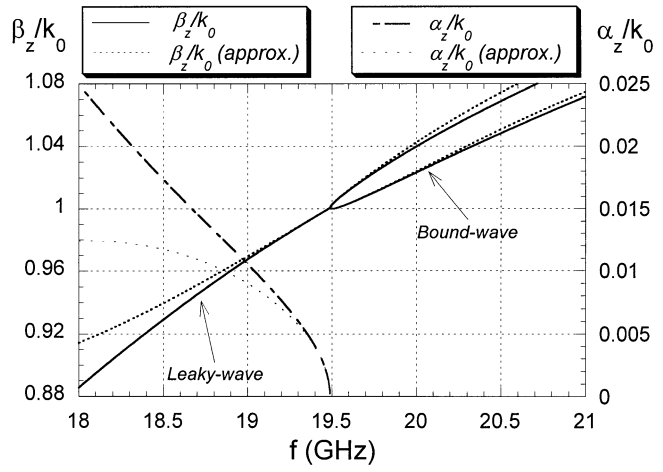

(a)

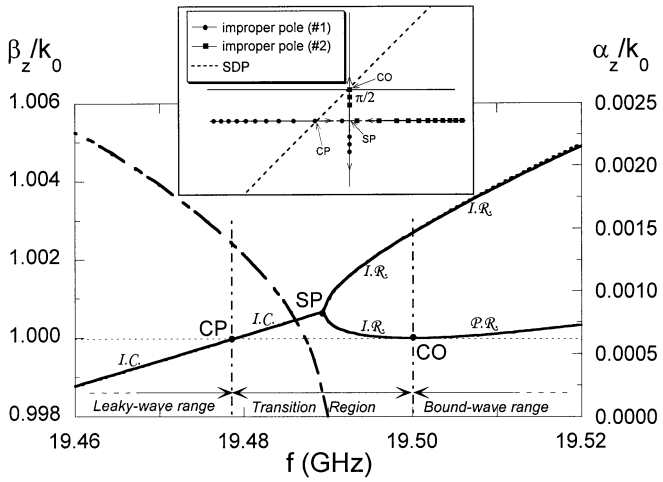

(b)

Fig. 3. Comparison between the exact and approximate poles of the Green's function, as a function of frequency, for a structure as in Fig. 1 with $\varepsilon_{r1} = 2.1$, $\mu_{r1} = 1$; $\varepsilon_{r2} = 10.8$, $\mu_{r2} = 1$, optimized for $\theta_p = \pi/2$, at a frequency of 19.5 GHz. (a) Comparisons between exact and approximate values for the normalized phase (β_z/k_0) and attenuation (α_z/k_0) constants. (b) Detail of the transition region between the TE_2 LW and TE_2 bound-wave ranges. Point labels: CP: crossing point; SP: splitting point; CO: cutoff. Curve labels: I.C.: improper complex; I.R.: improper real; P.R.: proper real. In the inset figure, the relevant pole locations in the steepest descent plane are also shown; the arrows on the axes indicate the direction of pole migration as frequency increases.

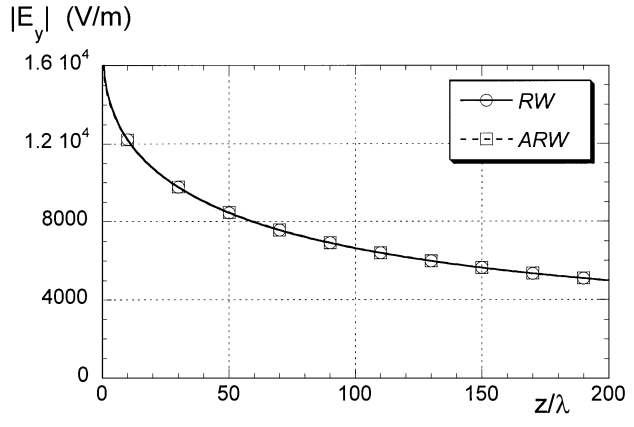

(a)

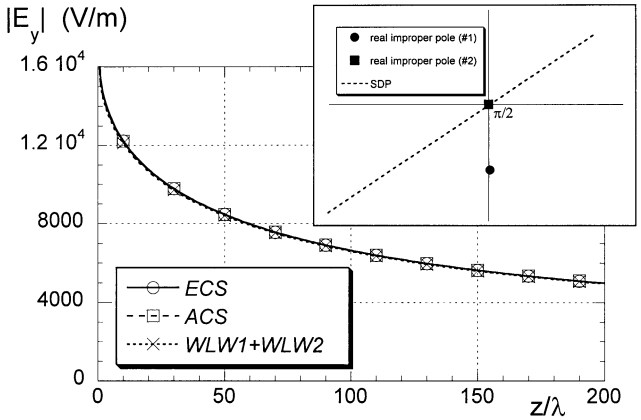

(b)

Fig. 4. Electric-field magnitude on the air–dielectric interface as a function of the normalized distance z/λ for the structure in Fig. 3 at the cutoff frequency $f_{\mathrm{co}} = 19.5$ GHz. (a) Exact RW and ARW. (b) ECS, ACS, and the weighted LW field (WLW1 + WLW2). In the inset figure, the location of the relevant poles in the steepest descent plane is shown.

IV. Numerical Results and Discussion

To demonstrate the validity of the proposed formulation, different numerical results will be presented for the structure of Fig. 1, with parameters as in the caption of Fig. 3, in the presence of an electric source, optimized according to (1) for radiation at endfire $(\theta_p = \pi/2)$ at a frequency $f = 19.5$ GHz. For this scan angle, the TE_2 mode is exactly at cutoff.

In Section IV-A, results are reported for the near field; various frequencies are considered, both inside and outside the transition region of the involved TE_2 mode. In Section IV-B, the corresponding results for the far field are considered.

A. Near Field

To assess the accuracy of our approximate representation of the Green's function, we show in Fig. 3 a comparison between the exact poles $k_{z\mathrm{LW1}}$ and $k_{z\mathrm{LW2}}$ and the approximate poles s_1 and s_2 [see (11)] in a frequency range centered on the TE_2 cutoff frequency $f_{\mathrm{co}} = 19.5$ GHz. In particular, in Fig. 3(a), the exact and approximate normalized phase (β_z/k_0) and attenuation (α_z/k_0) constants are reported between 18 and 21 GHz for both poles, where $k_z = \beta_z - j\alpha_z$. In Fig. 3(b), a magnified scale is used, and the leaky- and bound-wave regimes of the TE_2 mode are explicitly indicated, separated by the transition region. The relevant pole locations in the steepest descent plane [6] are also reported in the inset figure.

The transition region begins at the frequency for which the complex improper leaky pole $k_{z\mathrm{LW1}}$ is no longer captured by the integral-path deformation [the crossing-point frequency labeled CP in Fig. 3(b)]. By increasing the frequency, the complex improper pole $k_{z\mathrm{LW1}}$ joins its complex conjugate $k_{z\mathrm{LW2}}$ [at the splitting-point frequency, labeled SP in Fig. 3(b)]; at the SP frequency, a double improper real pole exists, which splits into two distinct improper real poles at higher frequencies. At the cutoff frequency [labeled CO in Fig. 3(b)], one pole becomes *proper*, thus entering a bound-wave regime, while the other pole remains improper real; here, the transition region ends. It can be observed that, as expected, the agreement between exact and approximate dispersion curves is very good in a significant neigh-

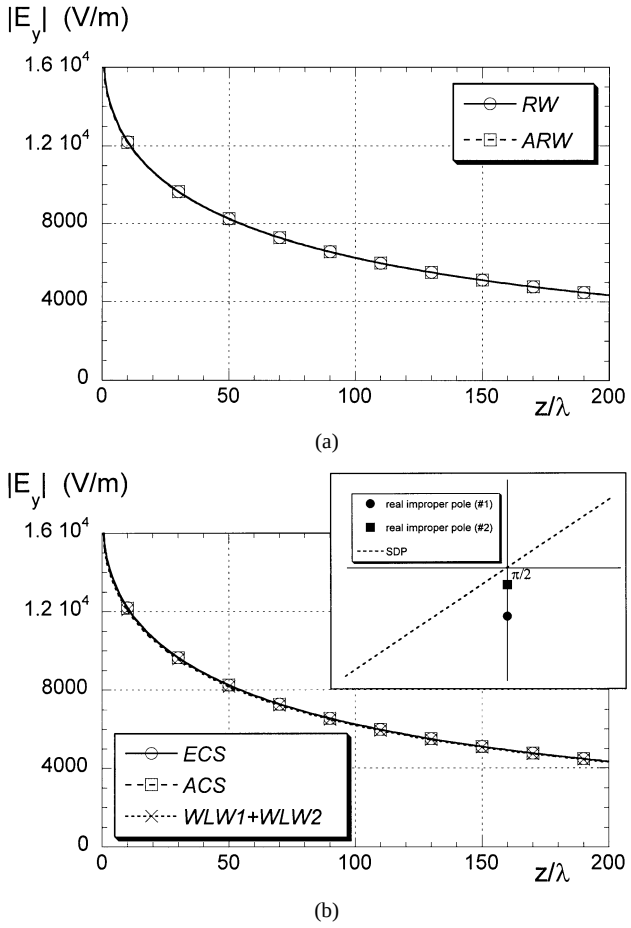

Fig. 5. Same as in Fig. 4, at the frequency $f = 19.493$ GHz, which is between the splitting-point and cutoff frequencies.

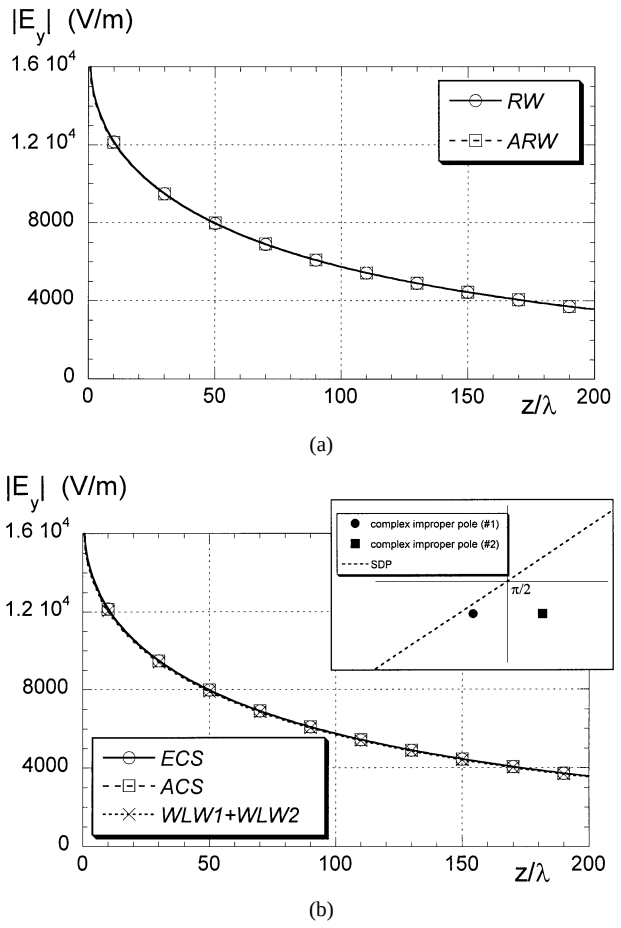

Fig. 6. Same as in Fig. 4, at the frequency $f = 19.484$ GHz, which is between the crossing- and splitting-point frequencies.

borhood of the transition region. In fact, the exact and approximate curves are essentially coincident in Fig. 3(b).

In Fig. 4, different results are reported for the electric field on the air–dielectric interface at the cutoff frequency $f_{\rm co} = 19.5$ GHz. In Fig. 4(a), a comparison is shown between the exact RW, calculated according to (5) by a numerical integration along the C_{k0} path, and our ARW formulation, calculated according to (13). The agreement is excellent, for z/λ (λ is the free-space wavelength) values down to unity, confirming that our approximate asymptotic representation is accurate and even close to the source. In Fig. 4(b), a comparison is shown among: 1) the exact continuous spectrum (ECS), calculated by subtracting the $\rm TE_1$ bound wave from the numerically evaluated TF; 2) the ACS evaluated according to (19) (using the approximate pole locations s_1 and s_2), which, in this case, is equal to the ARW alone; and 3) our weighted LW formulation (WLW1 + WLW2), calculated according to (21) (using the exact pole locations $k_{z\rm LW1}$ and $k_{z\rm LW2}$). Again, the agreement among the three curves is excellent. In the inset figure, the relevant location of the poles in the steepest descent plane is reported.

In Fig. 5(a) and (b), the same comparisons are shown at a frequency $f = 19.493$ GHz, for which the poles $k_{z\rm LW1}$ and $k_{z\rm LW2}$ are both real and improper [see the inset in Fig. 5(b)]. The agreement between the exact RWs and ARWs is again excellent, and our transition-function formulation (WLW1 + WLW2) again accurately represents the exact continuous-spectrum field. The same can be observed in Fig. 6(a) and (b), at a lower frequency $f = 19.484$ GHz, still inside the transition region, for which the poles $k_{z\rm LW1}$ and $k_{z\rm LW2}$ are a complex-conjugate pair, but $k_{z\rm LW1}$ is not yet captured.

By further lowering the frequency, the $\rm TE_2$ leaky pole is captured and directly contributes to the TF. In Fig. 7, comparisons are made at $f = 19.46$ GHz. It can be observed in Fig. 7(a) that the ARW is still very accurate. In Fig. 7(b), a comparison is shown among: 1) the ECS; 2) the ACS, which, in this case, is the sum of the exact LW field and the ARW field; 3) the result (WLW1 + WLW2); 4) the exact leaky field alone (LW); and 5) the ARW field alone. In this case, neither the LW, nor the ARW accurately represents the ECS; however, the ECS, ACS, and WLW1 + WLW2 results are almost completely superimposed.

Finally, in Fig. 8, the frequency $f = 18.5$ GHz is considered, for which the leaky $\rm TE_2$ pole is well captured and is far from the transition region. Once again, the RW is accurately represented by the ARW, even though its contribution to the total continuous spectrum ECS is negligible. In fact, in this case, the ECS is well represented by the LW (LW) alone, as can be seen in Fig. 8(b). The result WLW1 + WLW2 is still in very good agreement with the ECS, even slightly better than the LW field alone.

On the basis of the results presented thus far, it can be observed that the proposed representation of the continuous spectrum is very accurate over a wide frequency range, from fre-

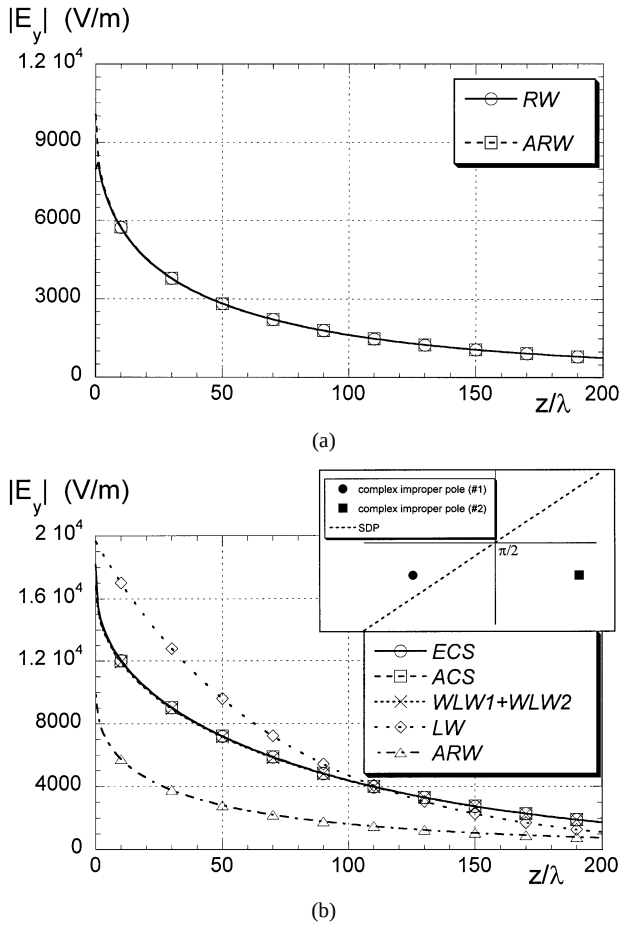

Fig. 7. Same as in Fig. 4, at the frequency $f = 19.46$ GHz, which is below the crossing-point frequency (the leaky-mode pole is physical). In (b), the exact LW field and ARW are also reported.

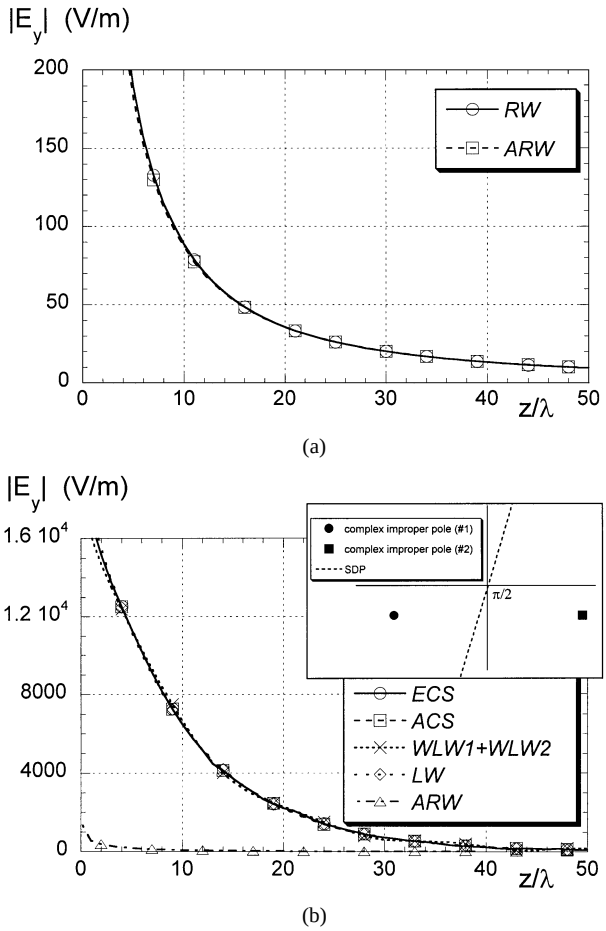

Fig. 8. Same as in Fig. 7, at the frequency $f = 18.5$ GHz, considerably below the crossing-point frequency (the leaky-mode pole is well within the physical region).

quencies where the LW is the dominant contribution to the continuous spectrum up to frequencies near cutoff, where the RW is instead the dominant contribution. In particular, it should be pointed out that, in the entire transition region, our formulation is an excellent representation of the continuous spectrum on the interface.

It must be stressed that, to obtain such a good agreement, the contribution of *two* poles had to be taken into account in the approximate representation of (21), where each term E_{LW1} and E_{LW2} is weighted by a transition function, which depends on both the frequency and longitudinal distance z. The contribution of both poles is important even though E_{LW2} always corresponds to a nonphysical pole that is never captured by the SDP deformation, and E_{LW1} may or may not correspond to a physical pole, depending on frequency.

It is interesting at this point to compare our formulation with a different empirical transition function, which is derived on the basis of power considerations proposed in [14] to accurately represent the radiated far field of the LW in the transition region. The transition function of [14] is real and independent of z; moreover, it is identically zero when the poles $k_{z\mathrm{LW1}}$ and $k_{z\mathrm{LW2}}$ are real and, therefore, it can be used only up to the splitting-point frequency. In Fig. 9, a comparison is shown among the ECS, exact TE_2 LW, weighted TE_2 LW (WLW1), and LW weighted by the empirical power-based leaky wave (PBLW) transition function of [14]. In particular, Fig. 9(a) is for a frequency inside the transition region ($f = 19.484$ GHz), where the leaky pole is not captured, while Fig. 9(b) is for a frequency at which the leaky pole $k_{z\mathrm{LW1}}$ is captured ($f = 19.46$ GHz). It can be observed that, in Fig. 9(a), none of the reported curves LW, WLW1, and PBLW agree with the ECS, thus confirming that, by taking into account just one leaky pole (i.e., the $k_{z\mathrm{LW1}}$ pole), it is never possible to achieve an accurate representation of the continuous-spectrum part of the near field when the leaky-mode pole is in the nonphysical region. When the leaky-mode pole is physical [see Fig. 9(b)], the fields LW and PBLW are in a reasonable overall agreement with the ECS. However, the agreement is not nearly as good as the agreement between the ECS and the sum of the WLW1 and WLW2 fields, which has been demonstrated previously.

It is interesting that the agreement between the ECS and the WLW1 field in Fig. 9(b) is not very good (although there is no reason why there should be agreement between these two fields since the ECS is approximated in our formulation as the sum of the WLW1 and WLW2 fields, and not the WLW1 field alone).

By displaying the absolute value of the continuous-spectrum field as a function of the normalized distance z/λ in a logarithmic scale at different frequencies (see Fig. 10), it can be seen that its asymptotic trend is always algebraic, with a $z^{-3/2}$ behavior at all frequencies, except at cutoff, where the behavior

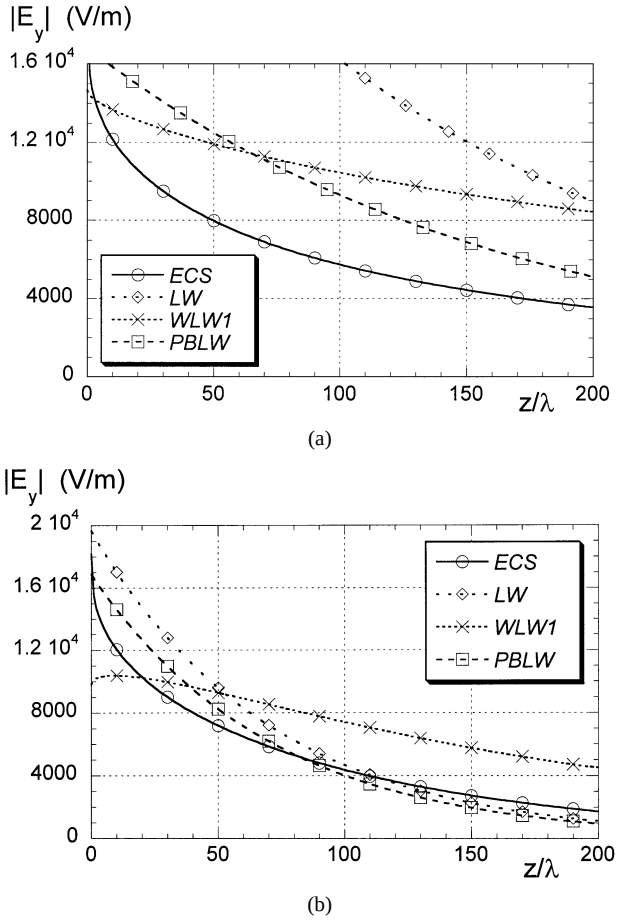

Fig. 9. Comparison of the magnitudes for the ECS, exact LW field, weighted LW field of the k_{zLW1} pole (WLW1), and PBLW field of [14] at: (a) $f = 19.484$ GHz (between the crossing- and splitting-point frequencies) and (b) $f = 19.46$ GHz (below the crossing-point frequency).

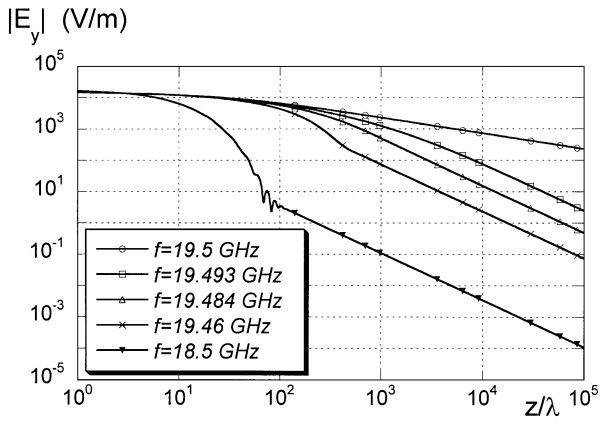

Fig. 10. Magnitude of the ACS field as a function of the normalized distance z/λ at different frequencies (corresponding to those considered in Figs. 4–9), plotted on a logarithmic scale.

is proportional to $z^{-1/2}$. Further, it can be noticed that, when the LW pole is captured (for $f = 19.46$ GHz and 18.5 GHz), the field has an exponential decay near the source; at 18.5 GHz, after the LW field has decayed to values comparable to those of the residual-wave field, the two fields interfere giving rise to oscillations; however, for higher z/λ values, the residual-wave field is always dominant, determining the algebraic asymptotic decay of the total continuous-spectrum field.

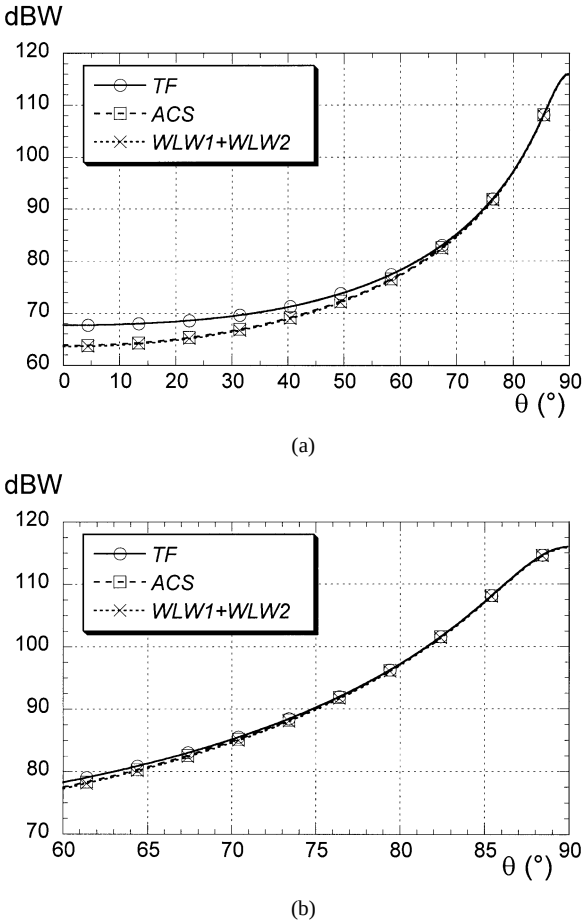

Fig. 11. (a) Power radiation patterns as a function of the angle θ (measured from broadside) for the structure in Fig. 4 ($f = f_{co} = 19.5$ GHz). Legend: TF: total field; ACS: approximate continuous spectrum; WLW1 + WLW2: weighted LW form of the ACS field. (b) Detail of the angular range near endfire.

B. Far Field

The same comparisons already shown for the electric field on the air–superstrate interface are reported in the subsequent figures for the radiated far field. In Fig. 11(a), the power radiation pattern at $f = f_{co} = 19.5$ GHz is shown for the TF, calculated by Fourier transforming the total aperture field, the radiation pattern obtained from Fourier transforming the ACS, and the radiation pattern obtained from Fourier transforming the field (WLW1 + WLW2), according to (25). The agreement is excellent near the main-beam direction, which occurs in this case at endfire ($\theta = 90°$), as is more clearly visible in the enlarged plot of Fig. 11(b).

In Fig. 12(a) and (b), the same comparisons are shown at $f = 19.493$ GHz and $f = 19.484$ GHz, respectively, both inside the transition region. Again, the agreement is excellent near the main-beam direction, which, in these cases, is very close to the endfire ($\theta \cong 88°$). In Fig. 13(a) and (b), the same comparisons are reported at $f = 19.46$ GHz and $f = 18.5$ GHz, respectively, both below the crossing point; in this case, we also show the radiation patterns of the exact LW field. It can be seen that, at $f = 19.46$ GHz, the LW pattern does not accurately represent the TF pattern, while both ACS and WLW1 + WLW2 do; in this case, the main-beam direction occurs at $\theta \cong 86°$. At

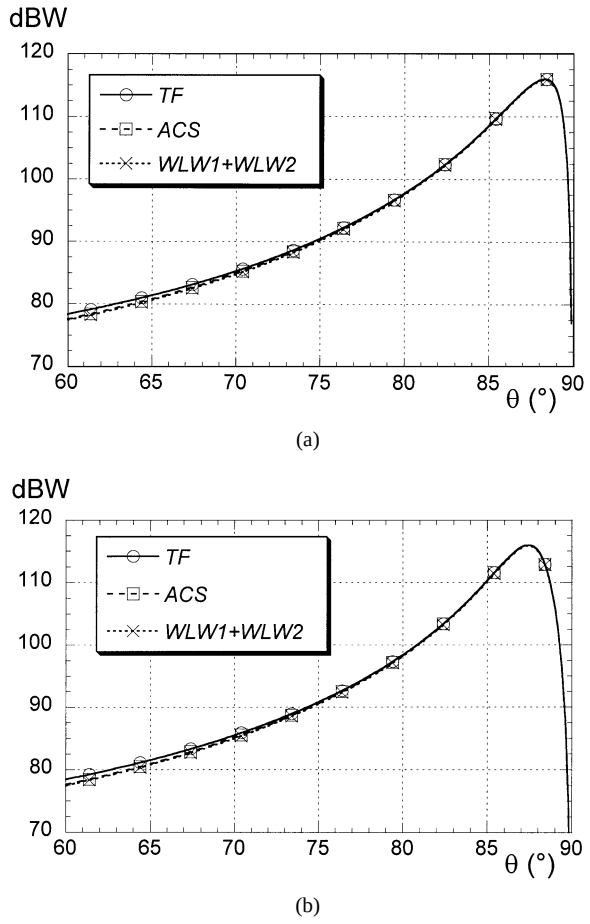

Fig. 12. Same as Fig. 11(b) at: (a) $f = 19.493$ GHz (between splitting-point and cutoff frequencies) and (b) $f = 19.484$ GHz (between the crossing- and the splitting-point frequencies).

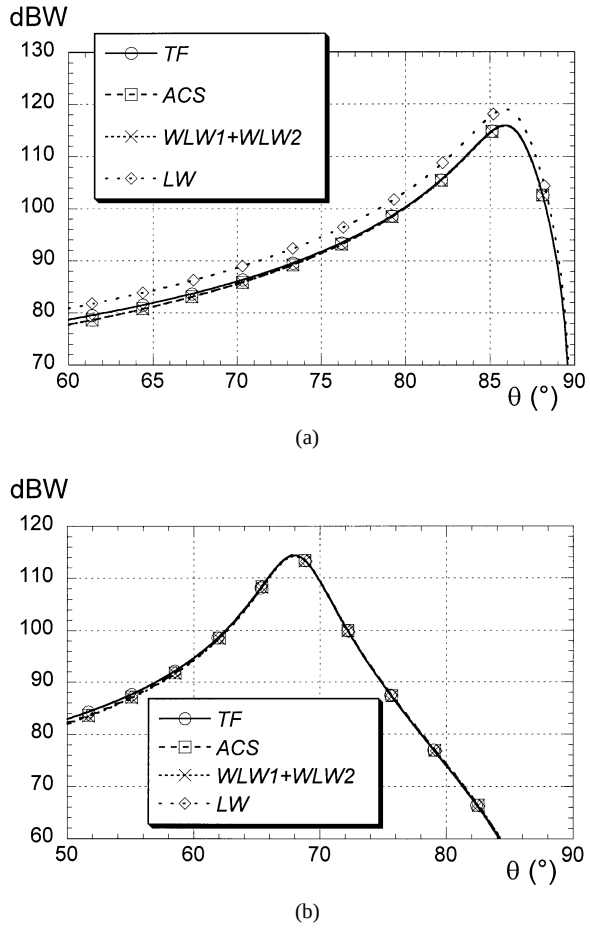

Fig. 13. Same as Fig. 11(b) at: (a) $f = 19.46$ GHz and (b) $f = 18.5$ GHz (both below the crossing-point frequency, where the leaky-mode pole is physical). For these frequencies, the radiation pattern of the exact LW field is also reported.

$f = 18.5$ GHz, the LW pattern is now in good agreement with the TF pattern; again, however, our formulation is even more accurate over a wide angular range around the main-beam direction, which, in this case, occurs at $\theta \cong 67°$.

In all the examined cases, our formulation yields accurate results for the far field, with the exception of the broadside region. However, in the latter angular range, the radiated power is considerably less than that radiated in the main-beam direction; the discrepancy between the TF and our formulation (WLW1 + WLW2) is due to three distinct effects, i.e., the bound-wave contribution, higher order leaky-pole contributions, and the difference between the exact and ARW fields, which is appreciable for z/λ values below unity.

In Fig. 14, a comparison is shown among the far-field patterns based on the TF, exact TE_2 LW, weighted TE_2 LW (WLW1), and weighted TE_2 LW using the empirical power-based formulation of [14] (PBLW) at $f = 19.484$ GHz [as shown in Fig. 14(a)] and [as shown in Fig. 14(b)] at $f = 19.46$ GHz. As for the corresponding results in the near field (see Fig. 9), at both frequencies, neither LW, nor WLW1 agrees with the TF. However, the PBLW field accurately represents the radiated far field, as already observed in [14]. Therefore, although the PBLW formulation is not a good (or even a reasonable) approximation to the aperture field, it nevertheless provides a good approximation to the total radiated far field. This is not surprising. In fact, the transition function in [14] was thought of as the necessary weighting factor that, when multiplied by the leaky-mode pole residue, yielded a leaky-mode aperture field whose transform matched well (as well as possible) with the total far field. However, it is worth pointing out that the PBLW far-field formulation can be used only in the presence of complex leaky poles, i.e., for frequencies up to the splitting point, as it does not provide any useful result in that part of the spectral-gap region where the poles are improper real modes (corresponding to a main-beam direction very close to endfire). In contrast, the radiation pattern obtained from the proposed WLW1+ WLW2 formulation developed here remains accurate throughout the entire spectral-gap region.

V. Conclusions

An original closed-form approximate expression for the continuous-spectrum aperture field has been formulated for a two-layer dielectric leaky-mode waveguide excited by an electric line source. The continuous-spectrum field is represented in the form of a weighted sum of two leaky-pole contributions: one corresponds to the leaky mode that forms the physical radiating beam, and the other corresponds to the nonphysical complex-conjugate pole. Numerical results show that the closed-form approximation is accurate for the field on the

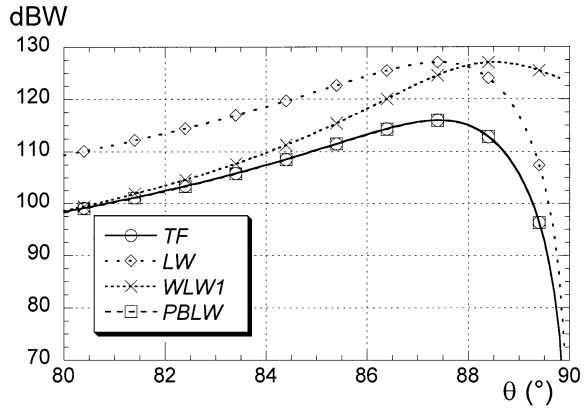

(a)

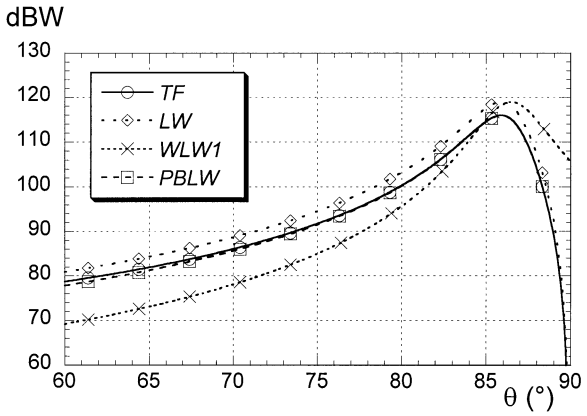

(b)

Fig. 14. Comparisons of the radiation patterns for the TF, exact LW field, weighted LW field of the $k_{z\mathrm{LW1}}$ pole (WLW1), and PBLW field of [14] at: (a) $f = 19.484$ GHz (between the crossing-point and the splitting-point frequencies) and (b) $f = 19.46$ GHz (below the crossing-point frequency).

aperture in the *entire transition region* of the relevant leaky mode. This new approximate closed-form expression for the continuous spectrum provides the opportunity to analytically explore the nature of the fields produced by a practical source in the transition region, as the leaky-mode pole moves through the spectral-gap region.

A closed-form approximate expression for the far field of the source was also obtained by analytically Fourier transforming the new closed-form approximate expression for the aperture field. The approximate far field was seen to be in excellent agreement with the exact far field. This new approximate formula for the far field was compared with one derived previously, which had been based on an empirical weighting of the leaky-mode aperture field. Although both approximations work well for a complex leaky mode, the new formula derived here works well throughout the entire spectral-gap region, including the region where the leaky mode has become an improper real mode. Furthermore, the formula developed here has been obtained from rigorous calculations, and not from empirical considerations.

Although formulated for a simple two-layer dielectric structure, many of the conclusions should remain valid for sources on practical microwave-integrated-circuit structures that support leaky modes.

APPENDIX

Here, the following integral will be evaluated in a closed form:

$$T(s_p,z)=\int_0^{+\infty}\frac{\sqrt{s}}{s-s_p}e^{-sz}ds. \tag{A.1}$$

By letting $t=sz$, we have

$$\begin{aligned}T(s_p,z)&=\int_0^{+\infty}\frac{\sqrt{\frac{t}{z}}}{\frac{t}{z}-s_p}e^{-t}\frac{dt}{z}\\&=\frac{1}{\sqrt{z}}\int_0^{+\infty}\frac{\sqrt{t}}{t-s_pz}e^{-t}dt\\&=\frac{1}{\sqrt{z}}T_1(s_pz)\end{aligned} \tag{A.2}$$

and, therefore, the main task consists in the evaluation of the following integral:

$$T_1(\Omega)=\int_0^{+\infty}\frac{\sqrt{t}}{t-\Omega}e^{-t}dt \tag{A.3}$$

where $\Omega=s_pz$. Through the variable substitution $u=\sqrt{t}$, where the square-root function is assumed to be evaluated according to the principal-value determination (with $-\pi/2\le\mathrm{Arg}[t]<3\pi/2$), we have

$$\begin{aligned}T_1(\Omega)&=\int_0^{+\infty}\frac{u}{u^2-\Omega}e^{-u^2}2udu\\&=2\int_0^{+\infty}\left[1+\frac{\Omega}{u^2-\Omega}\right]e^{-u^2}du\\&=\sqrt{\pi}-2\Omega\int_0^{+\infty}\frac{e^{-u^2}}{\Omega-u^2}du.\end{aligned} \tag{A.4}$$

By means of [20, eq. 7.1.4], we can write

$$\begin{aligned}T_1(\Omega)&=\sqrt{\pi}-(2\omega)\omega\int_0^{+\infty}\frac{e^{-u^2}}{\omega^2-u^2}du\\&=\sqrt{\pi}-2\omega\frac{\pi}{2j}e^{-\omega^2}\mathrm{Erfc}(-j\omega)\end{aligned} \tag{A.5}$$

where $\omega=\Omega^{1/2}$ with $\Im m[\omega]>0$, and

$$\mathrm{Erfc}(w)=\frac{2}{\sqrt{\pi}}\int_w^{+\infty}e^{-\xi^2}d\xi=1-\mathrm{Erf}(w). \tag{A.6}$$

In accordance with our previous definition (9) of the principal branch of the square-root function (denoted as $\sqrt{\cdot}$), we have $\omega=\pm\sqrt{\Omega}$, where the minus sign is chosen if Ω is located in the fourth quadrant on the complex plane; otherwise the plus sign is chosen.

From (A.5) and (A.6), we then have

$$\begin{aligned}T_1(\Omega)&=\sqrt{\pi}-\frac{\pi\omega}{j}e^{-\Omega}\big[1+\mathrm{Erf}(j\omega)\big]\\&=\sqrt{\pi}+j\pi\omega e^{-\Omega}\big[1+\mathrm{Erf}(j\omega)\big].\end{aligned} \tag{A.7}$$

Taking into account the relation between ω and Ω, and the fact that the Erf function is odd, we obtain

$$T_1(\Omega)=\sqrt{\pi}+j\pi\sqrt{\Omega}e^{-\Omega}\left[\pm1+\mathrm{Erf}\left(j\sqrt{\Omega}\right)\right] \tag{A.8}$$

where the lower sign is chosen if Ω lies in the fourth quadrant of the complex plane, otherwise the upper sign has to be chosen. Recalling the definition of Ω, we have

$$T(s_p,z)=\sqrt{\frac{\pi}{z}}+j\pi\sqrt{s_p}e^{-s_pz}\Big[\pm 1+\mathrm{Erf}\big(j\sqrt{s_pz}\big)\Big]. \tag{A.9}$$

With reference to the poles s_1 and s_2 of (11), it can easily be shown that

$$T(s_1,z)=\sqrt{\frac{\pi}{z}}+j\pi\sqrt{s_1}e^{-s_1z}\times\Big[\mathrm{Sgn}\big[\Im m[s_1]\big]+\mathrm{Erf}\big(j\sqrt{s_1z}\big)\Big] \tag{A.10}$$

$$T(s_2,z)=\sqrt{\frac{\pi}{z}}+j\pi\sqrt{s_2}e^{-s_2z}\Big[1+\mathrm{Erf}\big(j\sqrt{s_2z}\big)\Big] \tag{A.11}$$

where the imaginary part of the s_1 pole changes sign as the pole $k_{z\mathrm{LW1}}$ crosses the SDP.

REFERENCES

[1] V. V. Shevchenko, *Continuous Transitions in Open Waveguides*. Boulder, CO: Golem Press, 1971.

[2] R. E. Collin, *Field Theory of Guided Waves*. New York: IEEE Press, 1991, ch. 9.

[3] T. Rozzi and M. Mongiardo, *Open Electromagnetic Waveguides*. London, U.K.: IEE Press, 1997.

[4] G. W. Hanson and A. B. Yakovlev, *Operator Theory for Electromagnetics*. New York: Springer-Verlag, 2001.

[5] N. Marcuvitz, "On field representations in terms of leaky modes or eigenmodes," *IRE Trans. Antennas Propagat.*, vol. AP-4, pp. 192–194, July 1956.

[6] T. Tamir and A. A. Oliner, "Guided complex waves. Part I: Fields at an interface. Part II: Relation to radiation patterns," *Proc. Inst. Elect. Eng.*, vol. 110, pp. 310–334, Feb. 1963.

[7] L. Felsen and N. Marcuvitz, *Radiation and Scattering of Waves*. Englewood Cliffs, NJ: Prentice-Hall, 1973.

[8] L. B. Felsen, "Real spectra, complex spectra, compact spectra," *J. Opt. Soc. Amer. A, Opt. Image Sci.*, vol. 3, no. 4, pp. 486–496, Apr. 1986.

[9] M. J. Freire, F. Mesa, C. Di Nallo, D. R. Jackson, and A. A. Oliner, "Spurious transmission effects due to the excitation of the bound mode and the continuous spectrum on stripline with an air gap," *IEEE Trans. Microwave Theory Tech.*, vol. 47, pp. 2493–2502, Dec. 1999.

[10] D. R. Jackson, F. Mesa, M. J. Freire, D. P. Nyquist, and C. Di Nallo, "An excitation theory for bound modes, leaky modes, and residual-wave currents on stripline structures," *Radio Sci.*, vol. 35, no. 2, pp. 495–510, Mar.–Apr. 2000.

[11] P. Lampariello, F. Frezza, and A. A. Oliner, "The transition region between bound-wave and leaky-wave ranges for a partially dielectric-loaded open guiding structure," *IEEE Trans. Microwave Theory Tech.*, vol. 38, pp. 1831–1836, Dec. 1990.

[12] F. Mesa, D. R. Jackson, and M. J. Freire, "Evolution of leaky modes on printed-circuit lines," *IEEE Microwave Theory Tech.*, vol. 50, pp. 94–104, Jan. 2002.

[13] C. Di Nallo, F. Mesa, and D. R. Jackson, "Excitation of leaky modes on multilayer stripline structures," *IEEE Trans. Microwave Theory Tech.*, vol. 46, pp. 1062–1071, Aug. 1998.

[14] H. Ostner, J. Detlefsen, and D. R. Jackson, "Radiation from one-dimensional dielectric leaky-wave antennas," *IEEE Trans. Antennas Propagat.*, vol. 43, pp. 331–339, Apr. 1995.

[15] D. R. Jackson and N. G. Alexópoulos, "Gain enhancement methods for printed circuit antennas," *IEEE Trans. Antennas Propagat.*, vol. AP-33, pp. 976–987, Sept. 1985.

[16] D. R. Jackson and A. A. Oliner, "A leaky-wave analysis of the high-gain printed antenna configuration," *IEEE Trans. Antennas Propagat.*, vol. 36, pp. 905–910, July 1988.

[17] N. Bleistein and R. A. Handelsman, *Asymptotic Expansions of Integrals*. New York: Dover, 1986.

[18] M. Marin, S. Barkeshli, and P. H. Pathak, "Efficient analysis of planar geometries using a closed-form asymptotic representation of the grounded dielectric slab Green's function," *IEEE Trans. Microwave Theory Tech.*, vol. 37, pp. 669–679, Apr. 1989.

[19] M. Marin and P. H. Pathak, "An asymptotic closed-form representation for the grounded double-layer surface Green's function," *IEEE Trans. Antennas Propagat.*, vol. 41, pp. 1357–1366, Nov. 1992.

[20] *Handbook of Mathematical Functions*, 9th ed., M. Abramowitz and I. A. Stegun, Eds., Dover, New York, 1972.

Paolo Baccarelli (S'96–M'01) received the Laurea degree in electronic engineering and the Ph.D. degree in applied electromagnetics from the "La Sapienza" University of Rome, Rome, Italy, in 1996 and 2000, respectively.

In 1996, he joined the Department of Electronic Engineering, "La Sapienza" University of Rome. From April 1999 to October 1999, he was a Visiting Scholar with the University of Houston, Houston, TX. His research interests concern analysis and design of uniform and periodic planar LW antennas, numerical methods, and theoretical studies on LWs in anisotropic media.

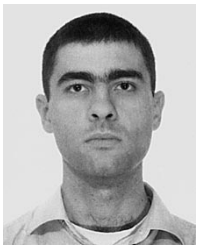

Paolo Burghignoli (S'98–M'01) was born in Rome, Italy, on February 18, 1973. He received the Laurea degree *(cum laude)* in electronic engineering and Ph.D. degree in applied electromagnetics from the "La Sapienza" University of Rome, Rome, Italy, in 1997 and 2001, respectively.

He is currently with the Department of Electronic Engineering, "La Sapienza" University of Rome. His scientific interests include analysis and design of planar LW antennas, general numerical methods for the analysis of passive guiding and radiating microwave structures, and inverse scattering theory.

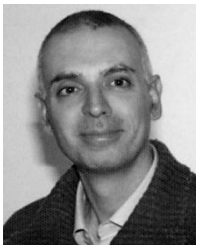

Fabrizio Frezza (S'87–M'90–SM'95) received the Laurea degree (*cum laude*) in electronic engineering and Doctorate degree in applied electromagnetics from the "La Sapienza" University of Rome, Rome, Italy, in 1986 and 1991, respectively.

In 1986, he joined the Electronic Engineering Department, "La Sapienza" University of Rome, where he has been a Researcher (1990–1998), a temporary Professor of electromagnetics (1994–1998), and, since 1998, an Associate Professor. His main research activity concerns guiding structures, antennas, and resonators for microwaves and millimeter waves, numerical methods, scattering, optical propagation, plasma heating, and anisotropic media.

Dr. Frezza is a member of Sigma Xi, the Electrical and Electronic Italian Association (AEI), the Italian Society of Optics and Photonics (SIOF), the Italian Society for Industrial and Applied Mathematics (SIMAI), and the Italian Society of Aeronautics and Astronautics (AIDAA).

Alessandro Galli (S'91–M'96) received the Laurea degree in electronic engineering and Ph.D. degree in applied electromagnetics from the "La Sapienza" University of Rome, Rome, Italy, in 1990 and 1994, respectively.

In 1990 he joined the Electronic Engineering Department, "La Sapienza" University of Rome, and became an Assistant Professor in 2000 and an Associate Professor in 2002. He currently teaches Electromagnetic Fields for Telecommunications Engineering. His scientific interests mainly involve electromagnetic theory and applications, particularly regarding the analysis and design of passive devices and antennas (dielectric and anisotropic waveguides and resonators, LW antennas, etc.) for microwaves and millimeter waves. He is also active in bioelectromagnetics (modeling of interaction mechanisms with living matter, health-safety problems for low-frequency applications and mobile communications, etc.).

Dr. Galli was the recipient of the 1994 and 1995 IEEE Microwave Theory and Techniques Society (IEEE MTT-S) Quality Presentation Recognition Award.

Giampiero Lovat (S'02) was born in Rome, Italy, on May 31, 1975. He received the Laurea degree (*cum laude*) in electronic engineering from the "La Sapienza" University of Rome, Rome, Italy, in 2001, and is currently working toward the Ph.D. degree in applied electromagnetics at the "La Sapienza" University of Rome.

His scientific interests include theoretical and numerical studies on leakage phenomena in planar structures and inverse scattering theory.

David R. Jackson (S'83–M'84–SM'95–F'99) was born in St. Louis, MO, on March 28, 1957. He received the B.S.E.E. and M.S.E.E. degrees from the University of Missouri, Columbia, in 1979 and 1981, respectively, and the Ph.D. degree in electrical engineering from the University of California at Los Angeles (UCLA), in 1985.

From 1985 to 1991, he was an Assistant Professor in the Department of Electrical and Computer Engineering, University of Houston, Houston, TX. From 1991 to 1998, he was an Associate Professor in the same department and, since 1998, he has been a Professor. His current research interests include microstrip antennas and circuits, LW antennas, leakage and radiation effects in microwave integrated circuits, periodic structures, electromagnetic compatibility (EMC), and bioelectromagnetics. He is an Associate Editor for the *International Journal of RF and Microwave Computer-Aided Engineering*. He was an Associate Editor for *Radio Science*.

Dr. Jackson is the chapter activities coordinator for the IEEE Antennas and Propagation Society (IEEE AP-S) and the chair of the Technical Activities Committee for URSI, U.S. Commission B. He is also a distinguished lecturer for the IEEE AP-S Society. He was an associate editor for the IEEE TRANSACTIONS ON ANTENNAS AND PROPAGATION. He is a past member of the IEEE AP-S Administrative Committee (AdCom).